Biochemistry and Biophysics Reports 38 (2024) 101724

Contents lists available at ScienceDirect

Biochemistry and Biophysics Reports

journal homepage: www.elsevier.com/locate/bbrep

Utility of pemafibrate in nonalcoholic steatohepatitis model mice induced by a choline-deficient, high-fat diet and dextran sulfate sodium

Takahiro Ota, Koichi Soga, Fuki Hayakawa, Mayumi Yamaguchi, Masaya Tamano *

Department of Gastroenterology, Dokkyo Medical University Saitama Medical Center, 2-1-50 Minami-Koshigaya, Koshigaya-shi, Saitama, 343-8555, Japan

ARTICLE INFO

Keywords:
Animal experimentation
Colitis
Fatty liver
Hepatitis
Liver cirrhosis
Tumorigenesis

ABSTRACT

Aim: The purpose of this study was to examine the effect of pemafibrate in a murine model of non-alcoholic steatohepatitis (NASH).

Methods: Forty-two, 19-week-old, male, C57BL/6J mice were divided into three groups: a Control group (n = 14), a dextran sulfate sodium (DSS) group (n = 14), and a DSS + PEM group (n = 14). All mice were given a standard rodent diet for the first week, followed by a choline-deficient, high-fat diet (CDHF) for the next 12 weeks. The 22nd day after the animals arrived was taken as Day 1 of the experiment. The Control group continued the CDHF diet and MilliQ water. The DSS group continued the CDHF diet, but starting on Day 1, the group received 0.8 % DSS to drink for 7 consecutive days, followed by MilliQ water for 10 days; this was taken as one course, and it was repeated on the same schedule until autopsy. The DSS + PEM group received the CDHF diet with PEM 0.1 mg/kg/day. Their drinking water was the same as that of the DSS group. On Seven animals from each group were autopsied on each of Day 50 and Day 120, and histopathological and immunohistochemical examinations, as well as quantitative RNA and cytokine measurements, of autopsied mice were performed.

Results: Pemafibrate improved hepatic steatosis (decreased steatosis area), improved liver inflammation enhanced by DSS (decreased aspartate transaminase and alanine aminotransferase), improved hepatic fibrosis promoted by DSS (decreased fibrotic areas and a marker of fibrosis), inhibited tumorigenesis, and decreased intestinal inflammation in the NASH model mice.

Conclusions: In a murine model of NASH, mixing PEM 0.1 mg/kg/day into the diet inhibited disease progression and tumor formation.

1. Introduction

Nonalcoholic steatohepatitis (NASH) is a condition in which inflammation and fibrosis of the liver occur due to the action of some secondary factor against a background of nonalcoholic fatty liver disease (NAFLD). NAFLD develops when fat is deposited in the liver in association with underlying diseases such as diabetes mellitus, dyslipidemia, and hypertension, and progression of NASH can lead to cirrhosis and liver cancer [1]. The prevalence of NAFLD is increasing worldwide with the rising prevalence of metabolic syndrome and obesity. In Japan, it increased from 25 % of the population in 2004 to 30 % in 2012, and it is predicted to reach 45 % by 2040 [2]. NASH is thought to account for 10–20 % of NAFLD, and the prevalence of NASH will likely increase as NFLD increases.

NASH is treated with diet and exercise therapy, in addition to which interventions to treat underlying diseases are also recommended [3]. It has been shown that progression to NASH can be slowed with treatment interventions for diabetes mellitus, dyslipidemia, hypertension, and other conditions [4–6]. However, all such interventions are effective only in reducing inflammation; they show no effect in inhibiting fibrosis or tumor expression in the tissue where that fibrosis originates. In that sense, no fundamental drug therapy has been established for NASH. Against this background, pemafibrate (PEM) is one drug that is currently attracting attention. PEM inhibits inflammation and fibrosis in NAFLD patients and has the potential to check its progression to NASH [7,8].

Several animal models have been developed for the study of NAFLD and NASH. The AMLN model is a diet-induced NASH model with methionine choline-deficiency (MCD), which exhibits the three stages of NAFLD (steatosis, steatohepatitis with fibrosis, and cirrhosis) without reliance on genetic mutations, the use of toxins, or nutrient deficiency

* Corresponding author. Department of Gastroenterology, Dokkyo Medical University Saitama Medical Center, 2-1-50 Minami-Koshigaya, Koshigaya-shi, Saitama, 343-8555, Japan.
E-mail address: mstamano@dokkyomed.ac.jp (M. Tamano).

https://doi.org/10.1016/j.bbrep.2024.101724
Received 23 February 2024; Received in revised form 22 April 2024; Accepted 26 April 2024

[9]. In a NASH model with diabetes mellitus (STAM model), created by exposing neonatal mice to low-dose streptozotocin (STZ) and giving them a high-fat diet, hepatocellular carcinoma developed at a high rate [10]. In recent years, a CDHF diet that combines a choline-deficient (CD) diet and an HF diet has been used to induce NASH, and carcinogenesis is seen in the liver on long-term observation in this model [11].

The purpose of this study was to examine the effect of PEM in a murine model of NASH. If inhibitory effects on inflammation, fibrosis, and tumor expression are shown in NASH model mice, this study could serve as a basis for future clinical application.

A two-hit hypothesis is considered the most likely the etiology of NASH [12]. Patients with NASH present increased intestinal permeability and small intestinal bacterial overgrowth, which correlate with the severity of steatosis [13]. So, intestinal inflammation caused by dextran sulfate sodium (DSS) may be the second hit in NASH. In the present study, we used the NASH model created with CDHF diet and DSS drinking based on a two-hit hypothesis [14].

2. Materials and methods

2.1. Animals and treatment

Forty-two, 19-week-old, male, C57BL/6J mice (SLC,Japan Shizuoka) were divided into three groups: a Control group, a DSS (MP Biomedical, Japan, Tokyo) group, and a DSS + PEM group. The mice were housed individually in cages in an environment with a regular 12-h light-dark cycle, temperature controlled at 18–26 °C, and humidity at 30–60 %. For the breeding acclimation, they were given MilliQ water to drink. The mice in all of the groups were given CLEA Rodent Diet CE-2 (A06071302) (CLEA JAPAN, Japan) as a standard diet for the first week for the same reason, followed by a choline-deficient, high-fat diet (CDHF) for the next 12 weeks. The standard diet contains 345 kcal per 100 g, of which the percentage of lipids is 12.47 % per calorie. On the other hand, CDHF diet contains 520.61 kcal per 100 g, of which the percentage of lipids is 61.7 % per calorie.

The 22nd day after the animals arrived was taken as Day 1 of the experiment. The Control group continued to be given the CDHF diet and MilliQ water. The DSS group continued to receive the CDHF diet, but starting on Day 1, the group was given 0.8 % DSS to drink for 7 consecutive days, followed by MilliQ water for 10 days [14]. The above was taken as one course, and this group repeated drinking DSS and MilliQ on the same schedule until autopsy. This schedule was repeated three and four times in Day 1–50 and Day 50–120. The DSS + PEM group was given the CDHF diet into which PEM 0.1 mg/kg/day was mixed [15,16]. Their drinking water was the same as in the DSS group (Fig. 1).

Seven animals from each group were autopsied on each of Day 50 and Day 120. For the autopsies, the animals were anesthetized with intraperitoneal administration of a combination of three anesthetics (medetomidine/midazolam/butorphanol, 0.3/4.0/5.0 mg/kg). After blood was collected from the inferior vena cava, the animals were euthanized by exsanguination. The liver, spleen, and large intestine were removed in the autopsy, and the weight of the liver and spleen and the total length of the large intestine were measured. These tissues were then fixed using 10 % neutral buffered formalin. The collected blood was used in biochemical analysis, and the liver, spleen, and colon were processed for histopathology. Part of the left lateral lobe of the liver was preserved in RNAlater solution. Serum was obtained by centrifuging for 15 min at 3000 g.

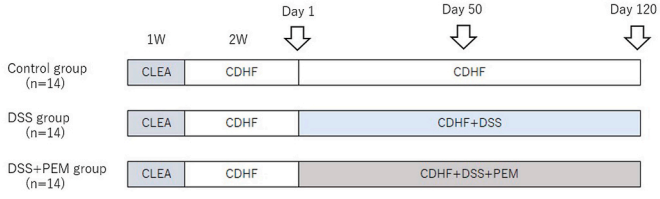

Fig. 1. Experimental methods
Mice in all groups are given a standard diet of CLEA for the first week, after which they are given a CDHF diet for 12 weeks. With the 22nd day as Day 1, the Control group continues to receive a CDHF diet and MilliQ. The DSS group continues to receive the CDHF diet, and from Day 1 is given 0.8 % DSS to drink for 7 consecutive days, followed by MilliQ drinking water for 10 days. This schedule was repeated three and four times in Day 1–50 and Day 50–120. In the DSS + PEM group, PEM 0.1 mg/kg/day is mixed into the CDHF diet, while drinking water is the same as in the DSS group.

The procedures used for the handling and care of animals were approved by the Animal Experiment Committee, Dokkyo Medical University (approved No. 1430), and conformed to ARRIVE guidelines and was carried out in accordance with the U.K. Animals (Scientific Procedures) Act, 1986 and associated guidelines, EU Directive 2010/63/EU for animal experiments.

2.2. Biochemical analysis

Aspartate transaminase (AST) and alanine aminotransferase (ALT) were measured in serum. The DRI-CHEM NX700V (Fujifilm, Japan, Tokyo) was used for the measurements.

2.3. Histology and immunohistochemistry

The diagnosis of NASH was made after considering fatty deposition, necrotic inflammatory changes, fibrosis by the HE-stained histopathological images of liver. And the colon injury was evaluated using the colon histological score.

After the livers and large intestines from each group of mice were removed, they were fixed in 10 % neutral buffered formalin and embedded in paraffin. Hepatic sections were cut from paraffin blocks for staining with hematoxylin and eosin and Picro-Sirius Red Stain (Scy Tek LABORATORIES INC., USA) (3-μm thick) for histological examination. Colon sections were cut for staining with hematoxylin and eosin (7-μm thick) for histological examination. For immunohistochemistry, samples were incubated overnight with anti-F4/80 antibody (A700-209, 1:500, Bethl Lab. America), followed by incubation with Histofine Simple Stain Mouse MAX-PO (Rabbit) (Nichirei, Japan) for 2 h. Antigen retrieval was performed by heating at 121 °C for 5 min in an autoclave with citrate buffer pH 6.0. F4/80 expression shows the activation of inflammatory macrophages in the liver.

The regions with fatty deposits, regions positive for Sirius red, and regions positive for F4/80 were measured using WinROOF image analysis software (Mitani Corporation, Tokyo, Japan). In making these measurements, blood vessel area and vascular wall portions were excluded.

Histological scoring was used to assess the large intestinal mucosa (× 100). Focally increased numbers of inflammatory cells in the lamina propria were scored as 1, with confluence of inflammatory cells extending into the submucosa scored as 2 and transmural extension of the infiltrate as 3.

For tissue damage, discrete lymphoepithelial lesions were scored as 1, mucosal erosions as 2, and extensive mucosal damage and/or extension through deeper structures of the bowel wall as 3.

The two equally weighted subscores (cell infiltration and tissue damage) were added, and the combined histological colitis severity score ranged from 0 to 6 [17].

2.4. RNA extraction and quantitative RNA analysis

Total RNA was extracted from tissues of the lateral left lobe of the liver saved in RNA later using ISOGEN (NIPPON GENE CO., Japan). Total RNA was isolated using the QuantiTect Reverse Transcription Kit (Qiagen, Germany) including an RNase-free DNAse step. The mRNA was quantified using the QuantStudio®5 real-time PCR system. TaqMan

probes (TNF-α, alpha-smooth muscle actin (SMA)) (ThermoFisher SCIENTIFIC, Japan), Housekeeping Genes (Gapdh) (Applied Biosystems, USA), and TaqPath qPCR Master Mix, CG (Applied Biosystems, USA) were used for quantification. TNF-α is inflammatory cytokine, and was measured for an index of liver inflammation, and α-SMA was measured for an index of liver fibrosis.

3. Method of cytokine measurement in colon tissue

A 2-cm-long segment of the colon was resected and immediately flash-frozen. Subsequently, the tissue was stored at −80 °C. Tissue extraction solution was prepared by adding a protease inhibitor (Thermo Scientific) (Cat: A32955) to RIPAbuffer (containing 50 mM Tris-HCl (pH 7.6), 150 mM NaCl, 0.5 % sodium deoxycholate, and 1 % TritonX-100). The colon tissue was homogenized using the tissue extraction solution. This liquid was used as samples for ELISA. IL-6 (Invitrogen) (Cat: BMS6002, BMS 603) levels were measured using the ELISA method.

3.1. Statistical analysis

Continuous data are expressed as means ± standard error of the mean (SEM). The Mann-Whitney test was used to compare each parameter in the three groups on Day 50 and on Day 120. The chi-squared test was used to compare tumorigenesis in the three groups. A *p* value of less than 0.05 was taken as a significant difference.

4. Results

4.1. Courses of body weight, liver to body weight, and spleen to body weight after DSS and CDHF diet administration

On Day 50, body weight was 28.55 g in the Control group, 24.76 g in the DSS group, and 23.96 g in the DSS + PEM group. The body weights were significantly lower in the DSS and DSS + PEM groups than in the Control group ($p < 0.05$, $p < 0.01$). No significant difference was seen between the DSS group and the DSS + PEM group. On Day 120, body weight was 31.14 g, 23.49 g, and 26.77 g, respectively. The DSS + PEM group was heavier than the DSS group ($p < 0.05$).

Liver/body weight (%) on Day 50 was higher in the DSS and DSS + PEM groups than in the Control group, but the difference was not significant. On Day 120, it was higher in the order of Control group, DSS + PEM group, and DSS group, with significant differences.

Spleen/body weight (%) tended to be high in the DSS group on both Day 50 and Day 120, but no significant differences were seen (Table 1).

4.2. Administration of pemafibrate improved hepatic steatosis after CDHF diet administration

Fatty changes in the liver parenchyma were assessed using hematoxylin-eosin (HE) stain. Hepatic tissue images from Days 50 and 120 are shown in Fig. 2A. The steatosis area (%) on Day 50 was 24.80 % in the Control group, 26.63 % in the DSS group, and 6.93 % in the DSS + PEM group. On Day 120, the steatosis area (%) was 24.57 %, 25.39 %, and 2.94 %, respectively. No significant difference was seen between the Control group and the DSS group on either Day 50 or Day 120, but the steatosis area was shown to be significantly lower in the DSS + PEM group than in the other two groups on both Days 50 and 120 ($p < 0.01$, Fig. 2B).

4.3. Administration of pemafibrate improved liver inflammation enhanced by DSS

Serum AST and ALT values were higher in the DSS group than in the Control group on both Days 50 and 120. The DSS + PEM group had significantly lower values than both the Control group and DSS group on both Days 50 and 120 (Table 1). On examination of histological images with HE stain, necrotic inflammatory changes in lobules were milder in the DSS + PEM group than in the Control group and DSS group (Fig. 2A).

On Day 50, TNF-α in liver tissue was 0.62 pg/mL in the Control group, 0.73 pg/mL in the DSS group, and 0.17 pg/mL in the DSS + PEM group. On Day 120, TNF-α was 0.95 pg/mL, 0.88 pg/mL, and 0.25 pg/mL, respectively. The values were lower in the DSS + PEM group on both Days 50 and 120 (Fig. 2C).

F4/80 immunohistochemical staining, which shows the activation of inflammatory macrophages, was also performed (Fig. 3A). The areas positive for F4/80 on Day 50 were 8.03 % in the Control group, 11.27 % in the DSS group, and 7.08 % in the DSS + PEM group. On Day 120, the areas positive for F4/80 were 9.96 %, 11.50 %, and 5.65 %, respectively. Thus, the DSS group showed higher values than the Control group on both Days 50 and 120. The DSS + PEM group showed significantly lower values than the DSS group on both Days 50 and 120 ($p < 0.01$, Fig. 3B).

4.4. Administration of pemafibrate improved hepatic fibrosis promoted by DSS

Hepatic fibrosis was assessed with Sirius red stain (Fig. 4A). On Day 50, the areas positive for Sirius red were 2.63 % in the Control group, 2.60 % in the DSS group, and 1.42 % in the DSS + PEM. On Day 120, the areas positive for Sirius red were 5.24 %, 16.73 %, and 6.00 %, respectively. Thus, on Day 50 there was no difference between the Control and DSS groups, whereas the DSS + PEM group had a significantly lower value than the other two groups ($p < 0.01$, $p < 0.05$). On Day 120, the value was significantly higher in the DSS group than in the

Table 1
CDHF + DSS-induced liver injury in mice.

	Day 50			Day 120		
	Control group (n = 7)	DSS group (n = 7)	DSS + PEM group (n = 7)	Control group (n = 7)	DSS group (n = 7)	DSS + PEM group (n = 7)
Body weight (g)	28.55 ± 0.72	24.76 ± 1.23*	23.96 ± 0.68***	31.14 ± 0.71	23.49 ± 0.88***	26.77 ± 1.14**
Liver/Body weight (%)	7.85 ± 0.54	9.25 ± 0.47	9.25 ± 0.31	8.39 ± 0.55	10.74 ± 0.36*	9.24 ± 0.43**
Spleen/Body weight (%)	0.77 ± 0.05	0.74 ± 0.10	0.59 ± 0.08	0.65 ± 0.03	0.81 ± 0.12	0.50 ± 0.07
Colon length (cm)	7.93 ± 0.16	6.77 ± 0.25*	6.41 ± 0.23***	8.01 ± 0.12	6.34 ± 0.28***	6.40 ± 0.29***
AST (IU/L)	279.8 ± 19.7	389.1 ± 12.0***	142.3 ± 17.0***&****	426.4 ± 25.7	624.0 ± 39.2***	65.0 ± 13.7***&****
ALT (IU/L)	278.6 ± 32.3	399.3 ± 11.4	111.0 ± 18.3***&****	562.9 ± 23.7	602.6 ± 57.5	195.0 ± 11.4***&****
Tumorigenesis	0/7	0/7	0/7	1/7	4/7	0/7**

Data are mean ± SEM values.
ALT, alanine aminotransferase: ALT, aspartate aminotransferase.
*$p < 0.05$ vs Control group.
**$p < 0.05$ vs DSS group.
***$p < 0.01$ vs Control group.
****$p < 0.01$ vs DSS group.

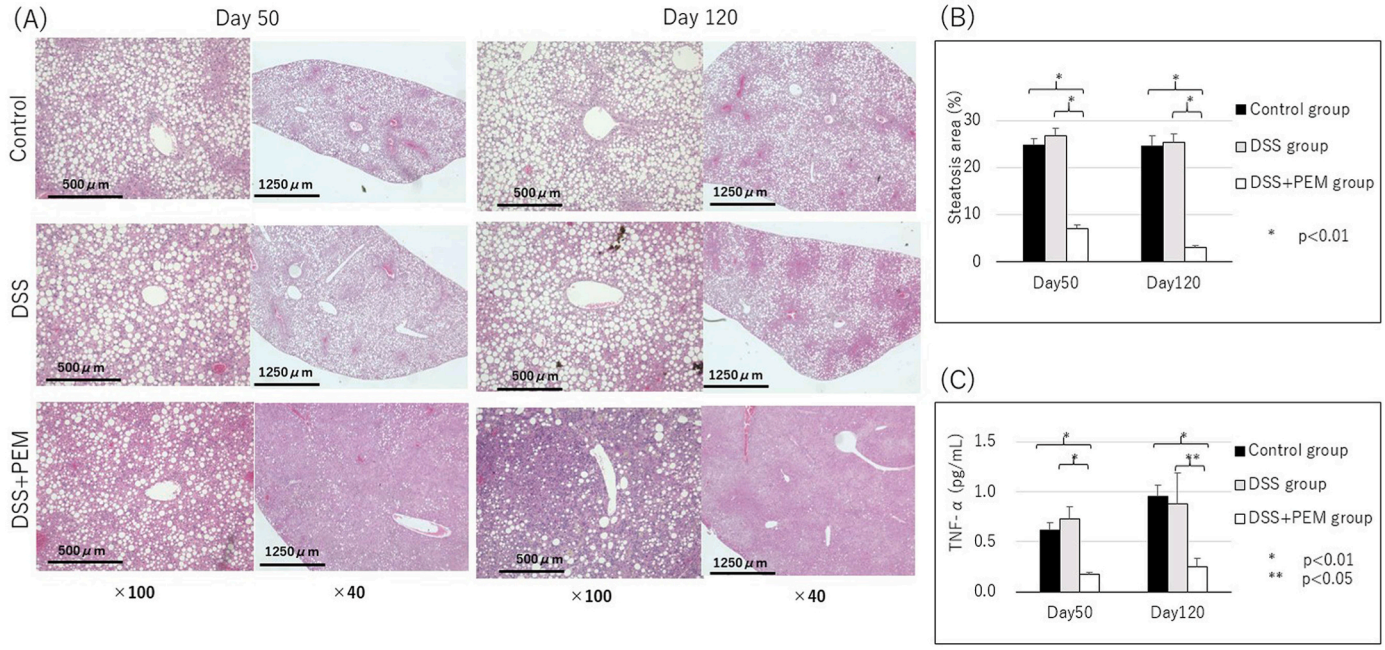

Fig. 2. Administration of pemafibrate improves hepatic steatosis and inflammation after CDHF diet administration.
A: HE-stained histopathological images of liver sampled at necropsy on Days 50 and 120 (× 100). On Day 50, fatty deposition is increased in the control group and the DSS group, with no inter-group difference. Levels on Day 50 are comparable to those on Day 120. Fatty deposits and necrotic inflammatory changes in the lobules are milder in the DSS + PEM group than in the Control and DSS groups. B: On Day 50, the steatosis area (%) is 24.80 % in the Control group, 26.63 % in the DSS group, and 6.93 % in the DSS + PEM group. On Day 120, the steatosis area (%) is 24.57 %, 25.39 %, and 2.94 %, respectively. No significant differences are seen between the Control and DSS groups on either Day 50 or Day 120, but the DSS + PEM group shows significantly lower values than the other two groups on both Days 50 and 120 ($p < 0.01$). C: On Day 50, TNF-α in liver tissue is 0.62 pg/mL in the Control group, 0.73 pg/mL in the DSS group, and 0.17 pg/mL in the DSS + PEM group. On Day 120, it is 0.95 pg/mL, 0.88 pg/mL, and 0.25 pg/mL, respectively. The values are lower in the DSS + PEM group on both Days 50 and 120 (Fig. 2C).

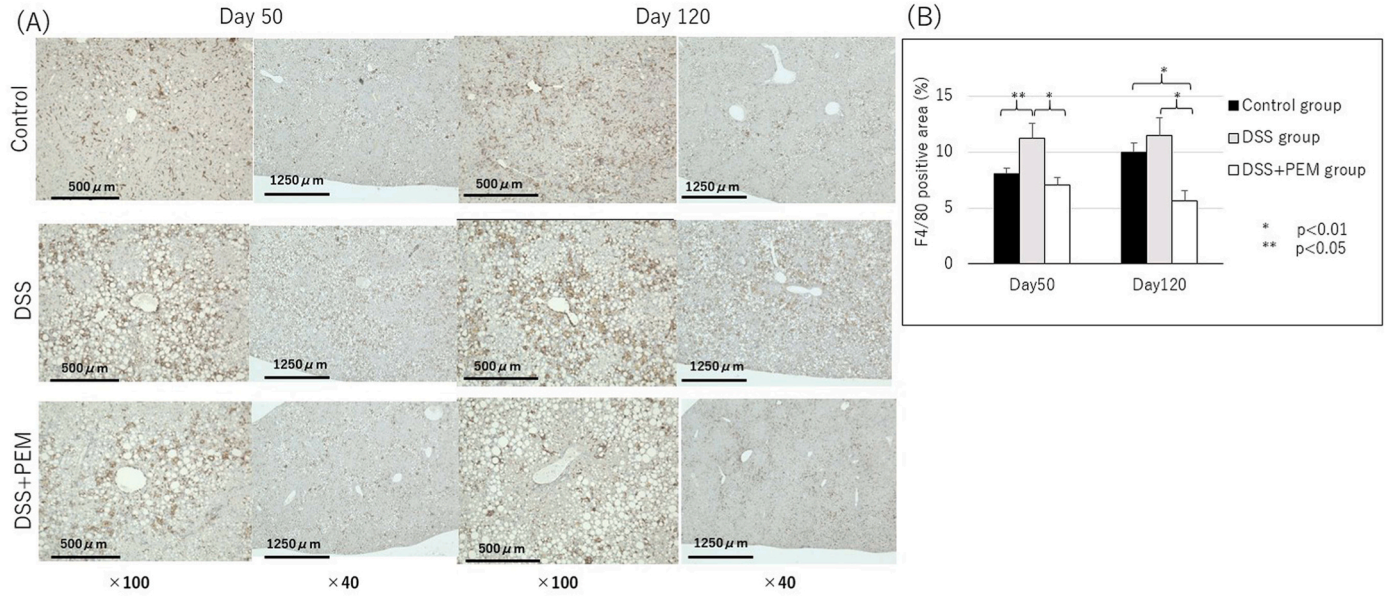

Fig. 3. Administration of pemafibrate improves activation of the inflammatory macrophage enhanced by DSS.
A: F4/80 immunohistochemical staining, which shows inflammatory macrophage activation, was performed (× 100). B: On Day 50, the F4/80 positive area is 8.03 % in the Control group, 11.27 % in the DSS, and 7.08 % in the DSS + PEM group. On Day 120, the F4/80 positive area is 9.96 %, 11.50 %, and 5.65 %, respectively. Thus, on both Days 50 and 120, the DSS group has higher values than the Control group. The DSS + PEM group shows significantly lower values than the DSS group on both Days 50 and 120 ($p < 0.01$).

Control group ($p < 0.01$). Meanwhile, the value was significantly lower in the DSS + PEM group than in the DSS group ($p < 0.01$), and no difference was seen with the Control group (Fig. 4B).

The level of α-SMA, a marker of liver fibrosis, was 1.09 pg/mL in the Control group, 1.07 pg/mL in the DSS group, and 0.35 pg/mL in the DSS + PEM group on Day 50. On Day 120, α-SMA was 1.18 pg/mL, 1.39 pg/mL, and 0.34 pg/mL, respectively. Thus, the DSS + PEM group showed significantly lower values than the other two groups on both Days 50

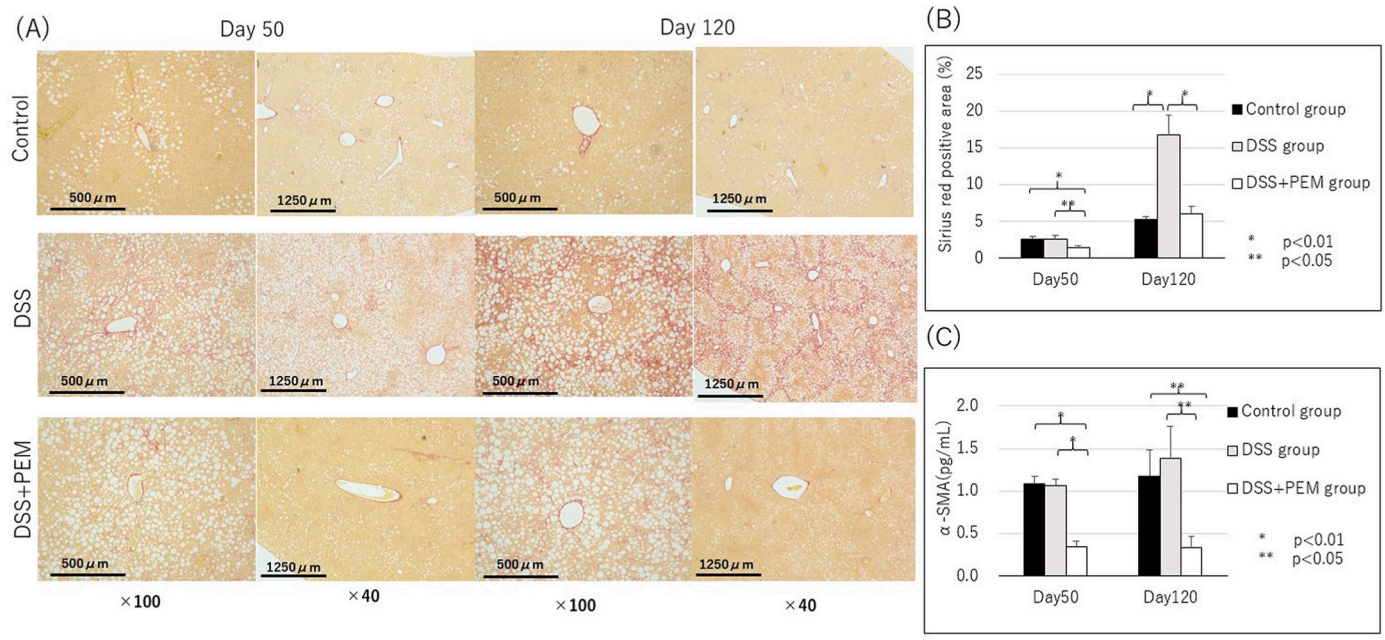

Fig. 4. Administration of pemafibrate improves hepatic fibrosis promoted by DSS.
A: Sirius red-stained histopathological images of liver samples from necropsy on Days 50 and 120 (× 100). B: On Day 50, the Sirius red-positive area is 2.63 % in the Control group, 2.60 % in the DSS group, and 1.42 % in the DSS + PEM group. On Day 120, it is 5.24 %, 16.73 %, and 6.00 %, respectively. Thus, on Day 50, there is no difference between the Control group and the DSS group, whereas the DSS + PEM group has a significantly lower value than the other two groups ($p < 0.01$, $p < 0.05$). On Day 120, the DSS group has a significantly higher value than the Control group ($p < 0.01$). Meanwhile, the DSS + PEM group shows a significantly lower value than the DSS group ($p < 0.01$) and no difference with the Control group. C: On Day 50, α-SMA is 1.09 pg/mL in the Control group, 1.07 pg/mL in the DSS group, and 0.35 pg/mL in the DSS + PEM group. On Day 120, α-SMA is 1.18 pg/mL, 1.39 pg/mL, and 0.34 pg/mL, respectively. Thus, on both Days 50 and 120, the DSS + PEM group shows significantly lower values than the other two groups ($p < 0.01$ on Day 50, $p < 0.05$ on Day 120; Fig. 4C). (For interpretation of the references to colour in this figure legend, the reader is referred to the Web version of this article.)

and 120 ($p < 0.01$ on Day 50, $p < 0.05$ on Day 120; Fig. 4C).

4.5. Administration of pemafibrate inhibited tumorigenesis induced by CDHF and DSS

Tumorigenesis was assessed with histological observation of the removed livers. On Day 50, no hepatic tumors were seen in any of the three groups. On Day 120, hepatic tumors were seen in 1 of 7 mice (14.3 %) in the Control group and 4 of 7 mice (57.1 %) in the DSS group, but no hepatic tumors were seen in any of the 7 mice in the DSS + PEM group (Table 1).

4.6. Intestinal inflammation after DSS administration

Histological changes in the colon were seen in the DSS group and the DSS + PEM group, and DSS exposure worsened histological findings, including crypt loss and an increased number of inflammatory cells, in the colon (Fig. 5A). On Day 50, the length of the large intestine was 7.93 cm in the Control group, 6.77 cm in the DSS group, and 6.41 cm in the DSS + PEM group. On Day 120, the length of the large intestine was 8.01 cm, 6.34 cm, and 6.40 cm, respectively. It was significantly shorter in the DSS group and the DSS + PEM group than in the Control group on both Days 50 and 120 (Table 1).

On Day 50, the colon histological score was 0.43 in the Control group, 2.14 in the DSS group, and 0.86 in the DSS + PEM group. On Day 120, the colon histological score was 0.56, 3.79, and 1.64, respectively. The colon histological score was significantly higher in both the DSS group and the DSS + PEM group than in the Control group on both Days 50 and 120 ($p < 0.01$). At the same time, it was significantly lower in the DSS + PEM group than in the DSS group ($p < 0.01$ in Day 50, $p < 0.05$ in Day 120; Fig. 5B).

The level of IL-6 in large intestinal tissue was 33.39 pg/mL in the Control group, 67.46 pg/mL in the DSS group, and 38.49 pg/mL in the DSS + PEM group on Day 50. On Day 120, IL-6 was 40.13 pg/mL, 82.89 pg/mL, and 48.93 pg/mL, respectively. Thus, it was higher in the DSS group than in the Control group, and a significant difference was seen on Day 120 ($p < 0.05$). The DSS + PEM group showed lower values than the DSS group, but no significant differences were seen on either Day 50 or Day 120 (Fig. 5C).

5. Discussions

The etiology of NASH is not fully understood, but a two-hit hypothesis is considered the most likely [12]. Conditions such as obesity, hypertension, hyperglycemia, and diabetes mellitus are the main causes of the first hit, in which fat is deposited in the liver (NAFLD). When NAFLD develops, the liver is susceptible to second hits from oxidative stress, iron deposition, endotoxins, mitochondrial dysfunction, lipid peroxidation, and pro-inflammatory cytokines [18–20].

DSS is a polymer of glucose which is sulfated from dextran, and the mean molecular weight is approximately 5000. DSS is used to create murine models of ulcerative colitis [21,22]. Exposure of the large intestinal mucosa to DSS through drinking water produces intestinal hyperpermeability and mucosal changes in the ileum and colon [23,24]. Intestinal inflammation causes the release of proinflammatory cytokines from enterocytes. There is a possibility of this being a second hit in a fatty liver model, and a NASH murine model created with use of both a CDHF diet and DSS drinking water has been reported [25–27]. In the present experiment, DSS drinking water was used with a CDHF diet to create a NASH model according to a report by Hayakawa et al. [14].

In the Control group and the DSS group, inflammation of the liver parenchyma was serologically and histopathologically confirmed, and TNF-α expression was increased. Staining with F4/80 immunohistochemical stain, which shows inflammatory macrophage activation,

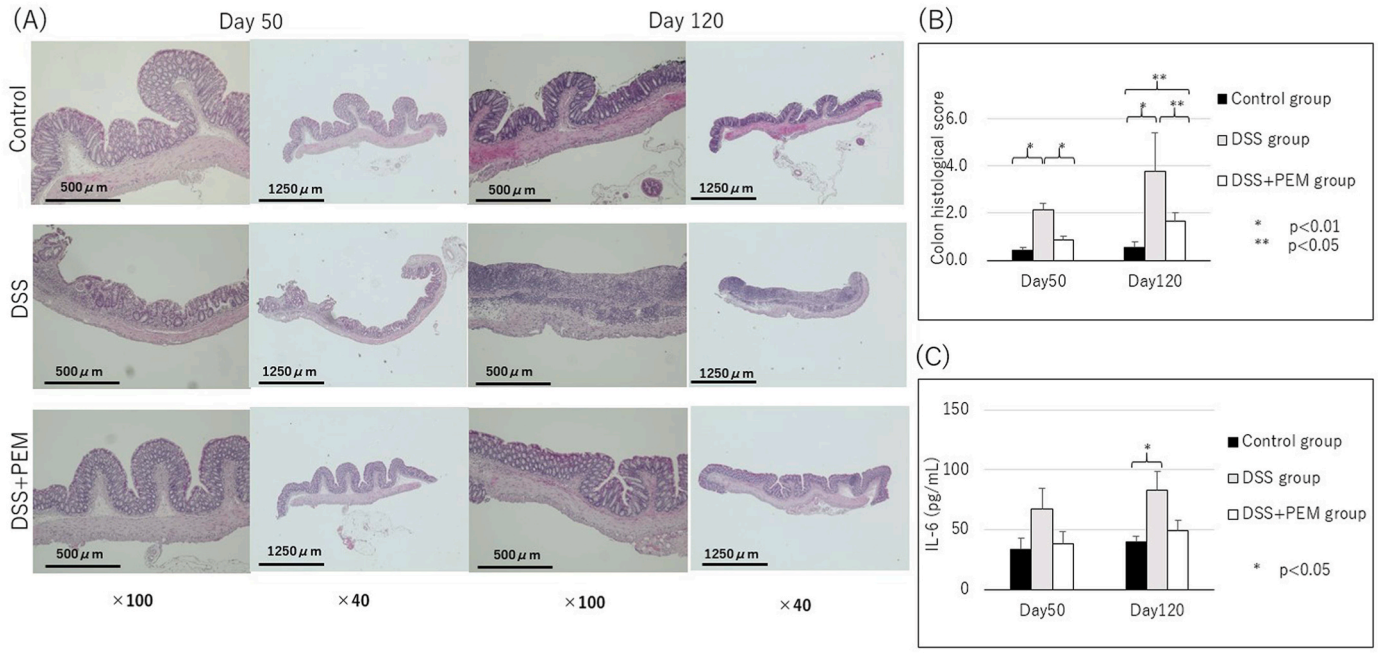

Fig. 5. Intestinal inflammation after DSS administration.
A: Histopathological images of large intestinal samples from necropsy on Days 50 and 120 (hematoxylin and eosin (H&E), × 40). Histological changes are seen in the DSS and DSS + PEM groups, and DSS exposure worsens histological findings, including crypt loss and an increased number of inflammatory cells in the colon (Fig. 5A). B: The colon histological score on Day 50 is 0.43 in the Control group, 2.14 in the DSS group, and 0.86 in the DSS + PEM group. On Day 120, it is 0.56, 3.79, and 1.64, respectively. On both Days 50 and 120, the colon histological score is significantly higher in both the DSS group and the DSS + PEM group than in the Control group ($p < 0.01$). At the same time, it is significantly lower in the DSS + PEM group than in the DSS group ($p < 0.01$ in Day 50, $p < 0.05$ in Day 120). C: On Day 50, IL-6 in large intestine tissue is 33.39 pg/mL in the Control group, 67.46 pg/mL in the DSS group, and 38.49 pg/mL in the DSS + PEM group. On Day 120, IL-6 is 40.13 pg/mL, 82.89 pg/mL, and 48.93 pg/mL, respectively. Thus, it is higher in the CDHF + DSS group than in the Control group, with a significant difference seen on Day 120 ($p < 0.05$). The DSS + PEM group shows lower values than the DSS group, but no significant differences are seen on either Day 50 or Day 120.

resulted in a higher positive area in the Control group and the DSS group, indicating that disruption of the large-intestinal mucosal barrier function contributed to liver inflammation. Evaluations of fibrosis showed a larger sirius red-positive area and higher α-SMA expression in the DSS group on Day 50 and 120.

On the other hand, steatosis area, TNF - α expression and F4/80 positive area significantly decreased in the PEM group on Day 50 and 120. And sirius red-positive area and α-SMA expression significantly decreased in the PEM group on Day 50 and 120.

PEM is a novel drug for the improvement of dyslipidemia that acts to lower the level of plasma triglycerides and increase HDL cholesterol by binding to peroxisome proliferator-activated receptor α (PPARα) and regulating the expression of target genes. It is known to have an anti-inflammatory effect on hepatocytes [28].

In NASH model mice, PEM has been reported to improve conditions such as obesity, dyslipidemia, and hepatic dysfunction. Honda et al., using the aforementioned AMLN model, showed that PEM facilitates the oxidation of fatty acids, resulting in increased ATP in the liver and accelerated lipid turnover. They also reported that stimulation of lipid turnover increases the expression of uncoupling protein 3 (UCP3) in the liver, contributing, at least in part, to improved oxidative capacity in mitochondria [29]. Sasaki et al. demonstrated that the administration of PEM in a STAM model facilitated the hydrolysis of triglycerides and esterification of fatty acids, and acted to inhibit the progression of NASH [30]. In the present model as well, these mechanisms are thought to have acted to inhibit the progression to NASH and the formation of tumors.

Meanwhile, in this NASH model, pro-inflammatory cytokines originating in the intestinal tract due to DSS also served as the second hit, and this is where the present study differs from the above two reports. Focusing on the colitis in this NASH model, it was seen that the length of the large intestine was significantly shorter in both the DSS group and the DSS + PEM group than in the Control group on both Days 50 and Day 120 (Table 1). The colon histological score was significantly higher in both the DSS group and the DSS + PEM group than in the Control group on both Day 50 and Day 120. This score was also significantly lower in the DSS + PEM group than in the DSS group (Fig. 5B). A similar trend was seen in the IL-6 level in large intestinal tissue, although there was no significant difference (Fig. 5C). The length of colon is an index of the rough colitis by the naked eye observation. The colon histological score and IL-6 content are the delicate index of colitis that we cannot determine with the naked eye. When both have estrangement, we give priority to the colon histological score and IL-6 content and should think.

Thus, in the present study, PEM was thought to have an inhibitory action on colitis induced by DSS. From the above, in a NASH model using a CDHF diet and DSS, PEM is conjectured to act both directly on the liver (first hit inhibition) and also in mitigating a second hit by inhibiting colitis, thereby inhibiting the progression of the disease and the formation of tumors.

Fenofibrate is a fibrate that is reported to exacerbate inflammation and tissue loss in a colitis model using DSS, with dependence on PPARα activation [31]. PEM is also a fibrate, and it activates PPARα more powerfully than does fenofibrate. Therefore, in the present study as well, there was some concern that colitis could be exacerbated with the administration of PEM. However, the effect was the opposite, and PEM was confirmed to have an inhibitory effect on DSS colitis.

As in ulcerative colitis models, DSS is administered in concentrations of 2–5% when the purpose is to create large intestinal lesions [32–34], which are higher concentrations than the 0.8 % in this model. It is not known at present whether the results in this study were due to differences in the concentration of DSS or whether PEM has some kind of inhibitory mechanism on DSS colitis. This is one question that we would like to investigate in the future.

5.1. Limitations

First, the assessment of cellular infiltration with HE staining was not an objective assessment. Immunohistochemical staining should have been used for these assessments.

Second, the mechanism of inhibition of DSS colitis with PEM was not elucidated. Investigations with DSS concentrations other than 0.8 % are perhaps necessary.

6. Conclusions

In a murine model of NASH created by CDHF diet and DSS, PEM inhibited disease progression and tumor formation. This is conjectured to be due to the effects of PEM in both a direct action on the liver (first hit inhibition) and in mitigating a second hit by inhibiting colitis.

Funding

This research did not receive any specific grant from funding agencies in the public, commercial, or not-for-profit sectors.

CRediT authorship contribution statement

Takahiro Ota: Methodology, Data curation. **Koichi Soga:** Formal analysis. **Fuki Hayakawa:** Data curation. **Mayumi Yamaguchi:** Data curation. **Masaya Tamano:** Methodology, Formal analysis.

Declaration of competing interest

The authors declare that they have no known competing financial interests or personal relationships that could have appeared to influence the work reported in this paper.

Acknowledgments

The authors would like to thank K. Fukuda and A. Takei of the Collaborative Research Center Dokkyo Medical University Saitama Medical Center, H. Tanaka and Y, Eda of the Research Center for Laboratory Animals Dokkyo Medical University Saitama Branch, and M Nakayama of Sankyo Labo Service Corporation, INC, for technical assistance with the experiments.

References

[1] Z.M. Younossi, A.B. Koenig, D. Abdelatif, Y. Fazel, L. Henry, M. Wymer, Global epidemiology of nonalcoholic fatty liver disease-Meta-analytic assessment of prevalence, incidence, and outcomes, Hepatology 64 (2016) 73–84, https://doi.org/10.1002/hep.28431.

[2] T. Ito, M. Ishigami, B. Zou, T. Tanaka, H. Takahashi, M. Kurosaki, M. Maeda, K. N. Thin, K. Tanaka, Y. Takahashi, Y. Itoh, K. Oniki, Y. Seko, J. Saruwatari, M. Kawanaka, M. Atsukawa, H. Hyogo, M. Ono, E. Ogawa, S.D. Barnett, C.D. Stave, R.C. Cheung, M. Fujishiro, Y. Eguchi, H. Toyoda, M.H. Nguyen, The epidemiology of NAFLD and lean NAFLD in Japan: a meta-analysis with individual and forecasting analysis, 1995-2040, Hepatol. Int. 15 (2021) 366–379, https://doi.org/10.1007/s12072-021-10143-4.

[3] K. Promrat, D.E. Kleiner, H.M. Niemeier, E. Jackvony, M. Kearns, J.R. Wands, J. L. Fava, R.R. Wing, Randomized controlled trial testing the effects of weight loss on nonalcoholic steatohepatitis, Hepatology 51 (2010) 121–129, https://doi.org/10.1002/hep.23276.

[4] S. Pelusi, S. Petta, C. Rosso, V. Borroni, A.L. Fracanzani, P. Dongiovanni, A. Craxi, E. Bugianesi, S. Fargion, L. Valenti, Renin-angiotensin system inhibitors, type 2 diabetes and fibrosis progression: an observational study in patients with nonalcoholic fatty liver disease, PLoS One 11 (2016) e0163069, https://doi.org/10.1371/journal.pone.0163069.

[5] P. Dongiovanni, S. Petta, V. Mannisto, R.M. Mancina, R. Pipitone, V. Karja, M. Maggioni, P. Kakela, O. Wiklund, E. Mozzi, S. Grimaudo, D. Kaminska, R. Rametta, A. Craxi, S. Fargion, V. Nobili, S. Romeo, J. Pihlajamaki, L. Valenti, Statin use and non-alcoholic steatohepatitis in at risk individuals, J. Hepatol. 63 (2015) 705–712, https://doi.org/10.1016/j.jhep.2015.05.006.

[6] H.B. El-Serag, T. Tran, J.E. Everhart, Diabetes increases the risk of chronic liver disease and hepatocellular carcinoma, Gastroenterology 126 (2004) 460–468, https://doi.org/10.1053/j.gastro.2003.10.065.

[7] H. Nomoto, K. Kito, H. Iesaka, T. Handa, S. Yanagiya, A. Miya, H. Kameda, K. Y. Cho, J. Takeuchi, S. Nagai, I. Sakuma, A. Nakamura, T. Atsumi, Preferable effects of pemafibrate on liver function and fibrosis in subjects with type 2 diabetes complicated with liver damage, Diabetol. Metab. Syndrome 15 (2023) 214, https://doi.org/10.1186/s13098-023-01187-7.

[8] A. Nakajima, Y. Eguchi, M. Yoneda, K. Imajo, N. Tamaki, H. Suganami, T. Nojima, R. Tanigawa, M. Iizuka, Y. Iida, R. Loomba, Randomised clinical trial: pemafibrate, a novel selective peroxisome proliferator-activated receptor α modulator (SPPARMα), versus placebo in patients with non-alcoholic fatty liver disease, Aliment Pharmacol. Therapeut. 54 (2021) 1263–1277, https://doi.org/10.1111/apt.16596.

[9] J.R. Clapper, M.D. Hendricks, G. Gu, C. Wittmer, C.S. Dolman, J. Herich, J. Athanacio, C. Villescaz, S.S. Ghosh, J.S. Heilig, C. Lowe, J.D. Roth, Diet-induced mouse model of fatty liver disease and nonalcoholic steatohepatitis reflecting clinical disease progression and methods of assessment, Am. J. Physiol. Gastrointest. Liver Physiol. 305 (2013) G483–G495, https://doi.org/10.1152/ajpgi.00079.2013.

[10] M. Fujii, Y. Shibazaki, K. Wakamatsu, Y. Honda, Y. Kawauchi, K. Suzuki, S. Arumugam, K. Watanabe, T. Ichida, H. Asakura, H. Yoneyama, A murine model for non-alcoholic steatohepatitis showing evidence of association between diabetes and hepatocellular carcinoma, Med. Mol. Morphol. 46 (2013) 141–152, https://doi.org/10.1007/s00795-013-0016-1.

[11] M.J. Wolf, A. Adili, K. Piotrowitz, Z. Abdullah, Y. Boege, K. Stemmer, M. Ringelhan, N. Simonavicius, M. Egger, D. Wohlleber, A. Lorentzen, C. Einer, S. Schulz, T. Clavel, U. Protzer, C. Thiele, H. Zischka, H. Moch, M. Tschöp, A. V. Tumanov, D. Haller, K. Unger, M. Karin, M. Kopf, P. Knolle, A. Weber, M. Heikenwalder, Metabolic activation of intrahepatic CD8+ T cells and NKT cells causes nonalcoholic steatohepatitis and liver cancer via cross-talk with hepatocytes, Cancer Cell 26 (2014) 549–564, https://doi.org/10.1016/j.ccell.2014.09.003.

[12] C.P. Day, O.F. James, Steatohepatitis: a tale of two "hits"? Gastroenterology 114 (1998) 842–845, https://doi.org/10.1016/s0016-5085(98)70599-2.

[13] L. Miele, V. Valenza, G. La Torre, M. Montalto, G. Cammarota, R. Ricci, R. Mascianà, A. Forgione, M.L. Gabrieli, G. Perotti, F.M. Vecchio, G. Rapaccini, G. Gasbarrini, C.P. Day, A. Grieco, Increased intestinal permeability and tight junction alterations in nonalcoholic fatty liver disease, Hepatology 49 (2009) 1877–1887, https://doi.org/10.1002/hep.22848.

[14] F. Hayakawa, K. Soga, J. Fujino, T. Ota, M. Yamaguchi, M. Tamano, Utility of ultrasonography in a mouse model of non-alcoholic steatohepatitis induced by a choline-deficient, high-fat diet and dextran sulfate sodium, Biochem. Biophys. Rep. 36 (2023) 101575.

[15] K. Murakami, Y. Sasaki, M. Asahiyama, W. Yano, T. Takizawa, W. Kamiya, Y. Matsumura, M. Anai, T. Osawa, J.C. Fruchart, J. Fruchart-Najib, H. Aburatani, J. Sakai, T. Kodama, T. Tanaka, Selective PPARα modulator pemafibrate and sodium-glucose cotransporter 2 inhibitor tofogliflozin combination treatment improved histopathology in experimental mice model of non-alcoholic steatohepatitis, Cells 11 (2022), https://doi.org/10.3390/cells11040720.

[16] K. Kanno, M. Koseki, J. Chang, A. Saga, H. Inui, T. Okada, K. Tanaka, M. Asaji, Y. Zhu, S. Ide, S. Saito, T. Higo, D. Okuzaki, T. Ohama, M. Nishida, Y. Kamada, M. Ono, T. Saibara, S. Yamashita, Y. Sakata, Pemafibrate suppresses NLRP3 inflammasome activation in the liver and heart in a novel mouse model of steatohepatitis-related cardiomyopathy, Sci. Rep. 12 (2022) 2996, https://doi.org/10.1038/s41598-022-06542-8.

[17] C. Bauer, P. Duewell, C. Mayer, H.A. Lehr, K.A. Fitzgerald, M. Dauer, J. Tschopp, S. Endres, E. Latz, M. Schnurr, Colitis induced in mice with dextran sulfate sodium (DSS) is mediated by the NLRP3 inflammasome, Gut 59 (2010) 1192–1199, https://doi.org/10.1136/gut.2009.197822.

[18] J.C. Cohen, J.D. Horton, H.H. Hobbs, Human fatty liver disease: old questions and new insights, Science (New York, N.Y.) 332 (2011) 1519–1523, https://doi.org/10.1126/science.1204265.

[19] T. Caballero, A. Gila, G. Sánchez-Salgado, P. Muñoz de Rueda, J. León, S. Delgado, J.A. Muñoz, M. Caba-Molina, A. Carazo, A. Ruiz-Extremera, J. Salmerón, Histological and immunohistochemical assessment of liver biopsies in morbidly obese patients, Histol. Histopathol. 27 (2012) 459–466, https://doi.org/10.14670/hh-27.459.

[20] F. Caballero, A. Fernández, A.M. De Lacy, J.C. Fernández-Checa, J. Caballería, C. García-Ruiz, Enhanced free cholesterol, SREBP-2 and StAR expression in human NASH, J. Hepatol. 50 (2009) 789–796, https://doi.org/10.1016/j.jhep.2008.12.016.

[21] F. Obermeier, N. Dunger, U.G. Strauch, C. Hofmann, A. Bleich, N. Grunwald, H. J. Hedrich, E. Aschenbrenner, B. Schlegelberger, G. Rogler, J. Schölmerich, W. Falk, CpG motifs of bacterial DNA essentially contribute to the perpetuation of chronic intestinal inflammation, Gastroenterology 129 (2005) 913–927, https://doi.org/10.1053/j.gastro.2005.06.061.

[22] I. Okayasu, S. Hatakeyama, M. Yamada, T. Ohkusa, Y. Inagaki, R. Nakaya, A novel method in the induction of reliable experimental acute and chronic ulcerative colitis in mice, Gastroenterology 98 (1990) 694–702, https://doi.org/10.1016/0016-5085(90)90290-h.

[23] S. Melgar, A. Karlsson, E. Michaëlsson, Acute colitis induced by dextran sulfate sodium progresses to chronicity in C57BL/6 but not in BALB/c mice: correlation between symptoms and inflammation, Am. J. Physiol. Gastrointest. Liver Physiol. 288 (2005) G1328–G1338, https://doi.org/10.1152/ajpgi.00467.2004.

[24] P.A. Dawson, S. Huxley, B. Gardiner, T. Tran, J.L. McAuley, S. Grimmond, M. A. McGuckin, D. Markovich, Reduced mucin sulfonation and impaired intestinal barrier function in the hyposulfataemic NaS1 null mouse, Gut 58 (2009) 910–919, https://doi.org/10.1136/gut.2007.147595.

[25] E. Gäbele, K. Dostert, C. Hofmann, R. Wiest, J. Schölmerich, C. Hellerbrand, F. Obermeier, DSS induced colitis increases portal LPS levels and enhances hepatic inflammation and fibrogenesis in experimental NASH, J. Hepatol. 55 (2011) 1391–1399, https://doi.org/10.1016/j.jhep.2011.02.035.

[26] K. Achiwa, M. Ishigami, Y. Ishizu, T. Kuzuya, T. Honda, K. Hayashi, Y. Hirooka, Y. Katano, H. Goto, DSS colitis promotes tumorigenesis and fibrogenesis in a choline-deficient high-fat diet-induced NASH mouse model, Biochem. Biophys. Res. Commun. 470 (2016) 15–21, https://doi.org/10.1016/j.bbrc.2015.12.012.

[27] M.Y. Wang, Z.X. Wang, L.J. Huang, R.X. Yang, Z.Y. Zou, W.S. Ge, T.Y. Ren, J. G. Fan, Premorbid steatohepatitis increases the seriousness of dextran sulfate sodium-induced ulcerative colitis in mice, J. Clinic. Translat. Hepatol. 10 (2022) 847–859, https://doi.org/10.14218/jcth.2021.00315.

[28] S. Ishibashi, S. Yamashita, H. Arai, E. Araki, K. Yokote, H. Suganami, J.C. Fruchart, T. Kodama, Effects of K-877, a novel selective PPARα modulator (SPPARMα), in dyslipidaemic patients: a randomized, double blind, active- and placebo-controlled, phase 2 trial, Atherosclerosis 249 (2016) 36–43, https://doi.org/10.1016/j.atherosclerosis.2016.02.029.

[29] Y. Honda, T. Kessoku, Y. Ogawa, W. Tomeno, K. Imajo, K. Fujita, M. Yoneda, T. Takizawa, S. Saito, Y. Nagashima, A. Nakajima, Pemafibrate, a novel selective peroxisome proliferator-activated receptor alpha modulator, improves the pathogenesis in a rodent model of nonalcoholic steatohepatitis, Sci. Rep. 7 (2017) 42477, https://doi.org/10.1038/srep42477.

[30] Y. Sasaki, M. Asahiyama, T. Tanaka, S. Yamamoto, K. Murakami, W. Kamiya, Y. Matsumura, T. Osawa, M. Anai, J.C. Fruchart, H. Aburatani, J. Sakai, T. Kodama, Pemafibrate, a selective PPARα modulator, prevents non-alcoholic steatohepatitis development without reducing the hepatic triglyceride content, Sci. Rep. 10 (2020) 7818, https://doi.org/10.1038/s41598-020-64902-8.

[31] Y. Qi, C. Jiang, N. Tanaka, K.W. Krausz, C.N. Brocker, Z.Z. Fang, B.X. Bredell, Y. M. Shah, F.J. Gonzalez, PPARα-dependent exacerbation of experimental colitis by the hypolipidemic drug fenofibrate, Am. J. Physiol. Gastrointest. Liver Physiol. 307 (2014) G564–G573, https://doi.org/10.1152/ajpgi.00153.2014.

[32] S. Yu, H. Guo, Z. Ji, Y. Zheng, B. Wang, Q. Chen, H. Tang, B. Yuan, Sea cucumber peptides ameliorate DSS-induced ulcerative colitis: the role of the gut microbiota, the intestinal barrier, and macrophage polarization, Nutrients 15 (2023), https://doi.org/10.3390/nu15224813.

[33] Z. Liu, J.R. Zhang, Y.X. Huang, X.Y. Li, H.P. Zhu, R.Y. Yang, S. Chen, Transcriptomic analysis reveals the regulatory mechanism underlying the indirubin-mediated amelioration of dextran sulfate sodium-induced colitis in mice, Pharmaceut. Biol. 61 (2023) 1082–1093, https://doi.org/10.1080/13880209.2023.2233565.

[34] L. Chen, X.L. Zhong, W.Y. Cao, M.L. Mao, D.D. Liu, W.J. Liu, X.Y. Zu, J.H. Liu, IGF2/IGF2R/Sting signaling as a therapeutic target in DSS-induced ulcerative colitis, Eur. J. Pharmacol. 960 (2023) 176122, https://doi.org/10.1016/j.ejphar.2023.176122.